An Examination of the Metallic Bonding of a Clad Material and Two Gold Plating Systems under Constant Force Fretting Conditions. 1.2

Neil Aukland~ Harry Hardee~ Anna Wehr~ Sean Brennan~ Philip Lees*

~ New Mexico State University
Advanced Interconnection Laboratory
PO Box 30001, MSC 3450
Las Cruces, NM 88003

* Technical Materials Inc.
Five Wellington Road
Lincoln, RI 02865

Abstract

Metallic bonding (cold welding) comparisons were made between a clad and two different gold plated contact materials under constant force fretting conditions. Previous experiments conducted at the Advanced Interconnections Laboratory showed that various material systems had different tendencies for metallic bonding. Three different material systems were selected to study this phenomenon. They were a thick gold plating, a gold flash over 80% palladium 20% nickel and a clad material (WE#1 over R156).

Four different normal forces: 20, 50, 100, and 200 grams were used in this research project. Contact resistance data were collected using a four-wire measurement system with the open circuit voltage limited to 0.02 volts. Relative humidity was controlled to be 40%. The procedure for each experiment was as follows: tangential force was increased until the static coefficient of friction was exceeded, then a constant displacement was maintained until a wear track was established, then a constant force was maintained throughout the remainder of the experiment. Two sets of data were collected during each experiment: fret amplitude and contact resistance.

The three material systems were statistically compared using analysis of variance techniques. They were compared on the number of fretting cycles needed to stop fretting motion, after a wear track was established.

Keywords: fretting, constant force, friction, clad, gold

1.0 Introduction

Whenever two clean metallic surfaces are pressed together, free electrons can move across the interface and form metallic bonds [1]. Highly conductive metals have many such free electrons [1]. The strength of these interfacial bonds is of the same order of magnitude as the bonds in a metallic crystal [1]. These bonds will increase in strength with time, due to the arrangement of atoms at the interface [1]. Soft metals tend to form metallic bonds so strong that chunks of metal will actually be torn from the surface, if moved [1].

Before fretting can occur, the two metal surfaces must experience a tangential force that exceeds the strength of the metallic bonds. There are two possible sources for this tangential force: thermal stress and vibration. The force due to thermal stress is:

$$Fs = A\,E\,n\,\Delta t$$

Where: A = area,
E = Young's modulus,
n = coefficient of thermal expansion,
Δt = temperature change [2].

The force due to vibration can be determined based on mass and acceleration. In either case, the tangential force must exceed the static coefficient of friction before fretting motion can occur.

Although the tendencies of connector material systems to form metallic bonds have been observed in the laboratory, basic research into the phenomenon has not been published. The goal of this research project is to begin to explore the tendency for a material system to form a strong metallic bond during fretting conditions.

2. Material Systems

Three different material systems were used in this research project. They were: a heavy gold system, a flash gold system and a clad material. All three systems used the same copper base metal. The alloy was UNS C17410 copper beryllium strip processed to the ½ HT temper. The heavy gold system consisted of 30 microinches of cobalt hardened gold plate, over 100 microinches of nickel. The flash gold system consisted of 3-5 microinches of cobalt hardened gold, over 40 micro-inches of 80% Pd - 20% Ni, over a 75 micro-inch layer of Ni. The percent of cobalt in the plated gold was 1%. Two different methods, atomic absorption spectrophotometry and gravimetric analysis, were used to verify the actual composition of the palladium-nickel layer. The result was 82% palladium and 18% nickel. The clad material system consisted of 10 microinches of 69% Au, 25% Ag, and 6% Pt (WE#1) over a 20 microinch layer of 60% Pd and 40% Ag (R156). Samples from the heavy gold system and clad system were sectioned. Individual layer thicknesses were verified to be within 8% of the quoted nominal values. The thickness of the flash gold layer was verified to be within tolerance using x-ray fluorescence.

The gold plating bath composition was gold potassium cyanide, citric acid and sodium citrate with a complexing agent and additive (Co). The pH level was held between 4 and 4.2. The temperature of the bath was 35° C. Current density was 0.5A/dm^2.

The palladium-nickel alloy plating bath composition was palladium (as metal in $PdCl_2$), nickel (as metal in $NiSO_4 \cdot 6H_2O$), $(NH_4)_2SO_4$) and hydroxycarboxylic acid. The pH level of this bath was 8.2. The temperature of the bath was 30° C. Current density was 3.0A/dm^2.

The Vickers hardness of each material system was measured at 20, 50, 100 and 200 gram loads. The values are listed in Table 1. The hardness of all material systems decreased by about 10% over the load range evaluated.

Table 1: Vickers hardness of the three material systems measured using various loads. Units are kg/mm^2.

Load (grams)	Material		
	Heavy Gold	Flash Gold	WE#1 over R156
20	254	254	169
50	254	249	155
100	238	243	155
200	232	231	150

The surface finish of each material system was evaluated by measuring both R_q and R_{MAX}. The results are listed in Table 2. WE#1 over R156 exhibited the smoothest surface. The gold flashed palladium-nickel exhibited a relatively smooth surface, but had a large maximum amplitude. The heavy gold samples exhibited a rougher surface and a larger amplitude.

3.0 Experimental Procedure.

Before motion can occur at the metallic interface, the tangential force must exceed the static coefficient of friction. After the static coefficient of friction is exceeded, the actual fret amplitude is very high. We

Table 2: Surface finish measurements for the three material systems. Units are micro-meters.

Material	Attribute	
	R_q	R_{MAX}
Hard gold	0.3	1.2
Flash gold	0.2	1.1
WE#1 over R156	0.1	0.5

found through preliminary experimentation that first the tangential force must exceed the static coefficient of friction, then the samples must be fretted in a constant displacement mode to establish a wear track. If a wear track is not established before the constant force mode begins, fretting motion will immediately stop. During the period that a wear track was being created, all of the contact resistance and fret amplitude data were collected. During the force driven period, only enough data were saved to visualize trends. Fret amplitude data were collected to determine the cycles required before the samples stopped moving (stick). At the end of every experiment, the samples were separated and the voltage and unloaded fret amplitude was recorded. This information was used in the calculation of the dynamic coefficient of friction.

All of the samples were cleaned using a commercially available contact solvent before each experiment. This contact cleaner contains isopropanol, ethanol, 2-methyl-2-propanol and carbon dioxide. Exact proportions are not given on the label. The manufacture advertises that the contact cleaner does not leave a residue.

3.1 Fretting machine

A force driven fretting machine was used for this research project. This fretting machine has been discussed in detail in previous publications [3,4] and can be used in either a constant force or a constant displacement mode. During each of the experiments in this research project, the fretting machine was used in a constant displacement mode and then in a constant force mode. A constant displacement was maintained by monitoring the fret amplitude and varying the power delivered to the electrodynamic drivers. Constant force fretting is accomplished by establishing a power level for a specific fret amplitude and then maintaining that power level throughout the rest of the experiment.

3.2 Contact geometry

For the hard gold and gold flashed palladium-nickel samples, narrow strips of copper were pre-formed followed by electroplating. The clad samples were formed after the cladding was applied.

The stationary component of a pseudo-crossed rod configuration was formed over a 9 mm diameter rod to make the "flat". The moveable component was dimpled with a 3 mm spherical diameter tool forming the " rider". The difference in radii of curvature was intentional. First, the contact of the two surfaces establishes a pseudo-crossed rod geometry and assures contact. This system was discussed in an earlier paper [4]. Second, during adhesive wear, for surfaces having no significant difference in hardness between the two surfaces, material is normally transferred from the flatter to the sharper surface. In this configuration, the surfaces of the mating components were identical and optical examination of the wear track on the "flat" provided a quick screening technique.

3.3 Contact Resistance Measurements

Contact resistance measurements were taken using a Hewlett Packard 4338A milliohmeter. This milliohmeter limited the open circuit ac voltage to 0.02 volt. Before each fretting experiment, the milliohmeter was zeroed through the pseudo-crossed rod configuration. This created a fixed reference point of zero resistance as the

Table 3: A list of the experimental conditions for the force driven study.

Experimental Set	Normal Force (grams)	Constant Displacement (cycles)	Fret Amplitude (microns)	Frequency (Hertz)
1	20.0	40.0	20.0	4.0
2	50.0	50.0	25.0	4.0
3	100.0	150.0	37.5	4.0
4	200.0	1000.0	67.5	4.0

initial value. Therefore, the contact resistance should initially go slightly negative as better metal to metal contact was made due to fretting motion.

3.4 Amplitude Measurements

The original fretting machine monitored fret amplitude using a single Keyence LC 2100 laser displacement meter. The target for this displacement meter was mounted on the moving rod in the crossed rod configuration. Another Keyence laser displacement meter was used to monitor the displacement on the stationary rod. The difference of the two displacement readings was used to calculate the relative motion at the metallic interface..

3.5 Experimental Conditions

One set of experimental conditions could not be established for all three material systems and for all four normal forces. Therefore, a different set of experimental conditions was established at each of the normal force levels. So, all three material systems were tested under the same conditions at each normal force level. These conditions are listed in Table 3. Each set of experimental conditions was replicated five times for each material system

4.0 Results and discussion

All of the fret amplitude data patterns were similar. Fret amplitude was stabilized at a selected value based on normal force during the constant displacement mode of each experiment. At the end of the constant displacement fretting cycles, the samples were fretted in a constant force mode. During the constant force mode, the fret amplitude would vary, probably due to changes in the levels of metallic bonding. All of the fret amplitude data sets had a common characteristic during the constant force regime. The fret amplitude would dip, increase, stabilize and suddenly decrease. Three characteristic fret amplitude data sets are shown in Figures 1, 2 and 3 for heavy gold, gold flashed palladium nickel and WE#1 over R156, respectively. All of the data in these figures were collected at 100 grams normal force.

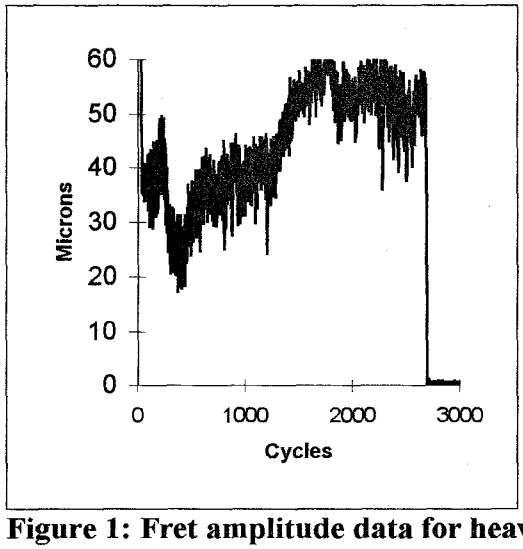

Figure 1: Fret amplitude data for heavy gold at 100 grams normal force.

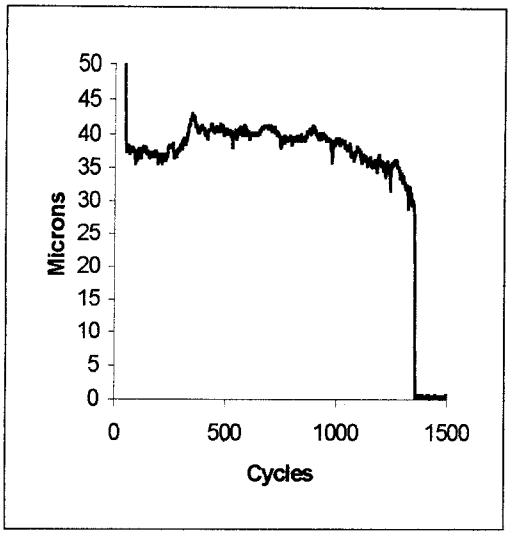

Figure 2: Fret Amplitude data for gold flashed palladium nickel at 100 grams normal force.

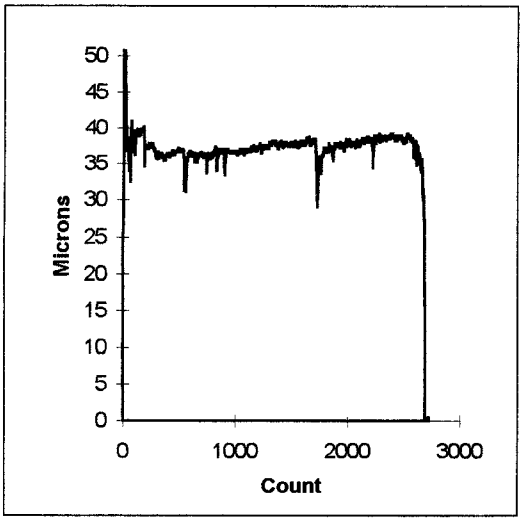

Figure 3: Fret amplitude data for WE#1 over R 156 at 100 grams normal force.

All of the contact resistance data had a similar pattern. Contact resistance would start at an initial value of approximately zero and steadily decrease throughout the remainder of the experiment. Figure 4 shows a contact resistance data set for gold flashed palladium nickel at 100 grams normal force. The overall conditions appear to be similar to Stage 1 of Bryant's model in

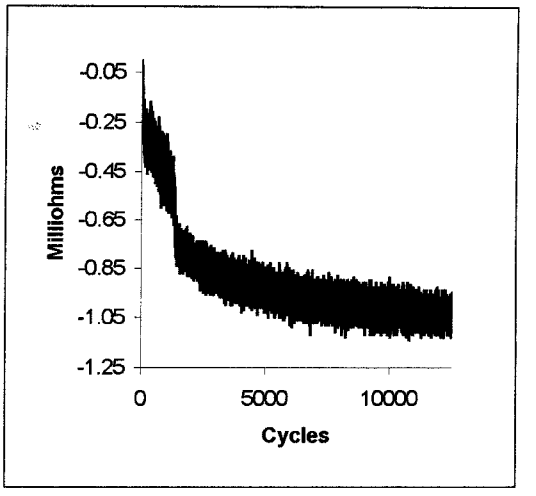

Figure 4: A contact resistance data set for gold flashed palladium nickel at 100 grams normal force.

which the contact resistance is steadily decreasing from an initial value [5].

One of the WE#1 over R156 experiments at 100 grams normal force was not stopped immediately after sticking. The data that was collected for this experiment is contained in Figure 5. The constant force fretting cycles were able to cause the sample to unstick and motion resumed, but at a smaller amplitude and for fewer cycles. This phenomena was observed by Waterhouse [6].

Figure 6 contains the contact resistance data set that correlates to the fret amplitude data in Figure 5. Some interesting observations can be made about contact resistance. First, contact resistance decreases throughout the entire experiment. Second if there is motion at the metallic interface, contact resistance values increase and have a larger variance. It is possible that the motion causes some aperities to lose contact, while new spots of contact are made at the asperity tips, which would explain the larger contact resistance variance during motion.

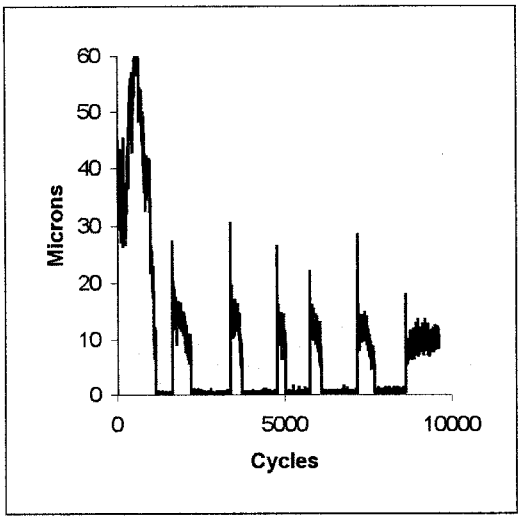

Figure 5: Another fret amplitude data set for WE#1 over R156 at 100 grams normal force.

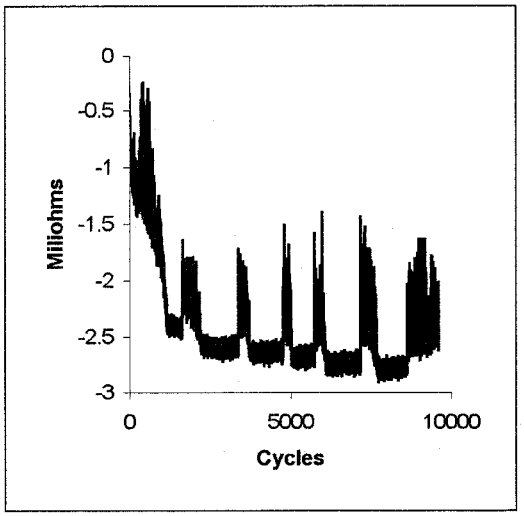

Figure 6: Contact resistance values for the data set in Figure 5.

A heavy gold sample was fretted under constant force conditions for an extended period at 200 grams normal force. The contact resistance data for this experiment is shown in Figure 7. Initially, contact resistance decreases rapidly as in Figure 4. Then the contact resistance values stabilize and a minimum is reached at approximately 850,000 cycles. The region after this minimum point is interesting because the contact resistance values are increasing. This increase in resistance may mean that some debris is forming in the metallic interface and causing the contamination of some of the touching asperity tips (Stage 2) [5]. Although no motion is detected during the first 1,600,000 constant force cycles, the asperity tips may be flexing. Moreover, some of the smallest asperity tips may even be making and breaking contact. The sharp increase in resistance at about 1,600,000 cycles is due to a short period of motion. These short periods of motion were discussed and are shown in Figure 5.

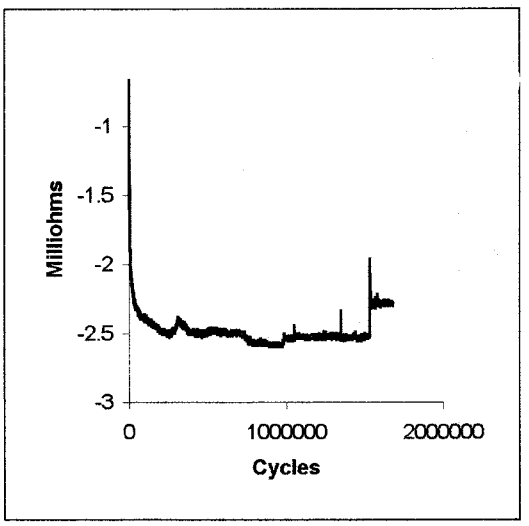

Figure 7: Contact resistance data for heavy gold at 200 grams normal force.

An overall statistical comparison between the experimental sets was not possible because the experimental conditions changed between sets. Therefore, analysis of variance techniques could only be conducted on each experimental set. A statistical comparison using linear contrasts was conducted for the material systems at each normal force. The only significant statistical comparison from this analysis was at 50 grams normal force. The linear contrast that compared heavy gold to the other two material systems was significant. All of the other statistical comparisons were inconclusive.

Because the statistical analysis was inconclusive, a simple graphing technique was used to look for trends in the data. An average was taken on the data for each material system at 20.0, 50.0, 100.0 and 200.0 grams normal force. A plot of this data is given in Figure 8. As expected, the heavy gold system maintained motion under constant force conditions for a longer period than the other two systems. Although the statistical comparison did not detect a significant difference between the clad and flash gold system, a trend can be seen in Figure 8. The clad material appears to be slightly less prone to weld when compared to the gold flashed palladium-nickel.

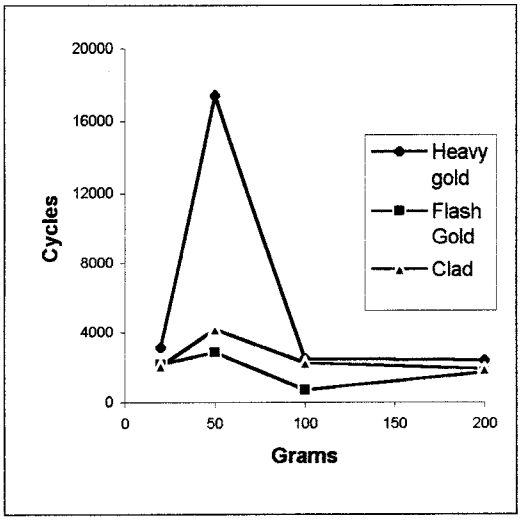

Figure 8: The average number of cycles required to cause the samples to stick for all three material systems.

The dynamic coefficient of friction can be used as a figure of merit in the comparison of different material systems. The tangential force developed by the fretting machine was modeled mathematically and simulated with a computer program. This development is lengthy and is presented in Appendix 1. The results of these simulations were used to calculate values for the dynamic coefficient of friction. The following data were collected for each experiment: the amplitude of motion, the amplitude of the sinusoidal voltage sent to the motion driver, the normal force on the fretting surface, and the contact resistance.

Using the model developed in Appendix 1 and the data collected at the end of each experiment, the dynamic coefficients of friction were calculated utilizing Equations (15) and (16) of Appendix 1. Figures 9, 10 and 11 contain friction force versus normal force data for heavy gold, flash gold and WE#1 over R156, respectively.

Linear regression was used to calculate the best-fit straight line through these data points. The slope of this line is actually the expected value of the dynamic coefficient of friction. Table 4 contains the expected coefficient of friction and the upper and lower values of the 95% confidence interval for each material system. These confidence intervals can be used to make conclusions about the differences in dynamic coefficient of friction between material systems. The

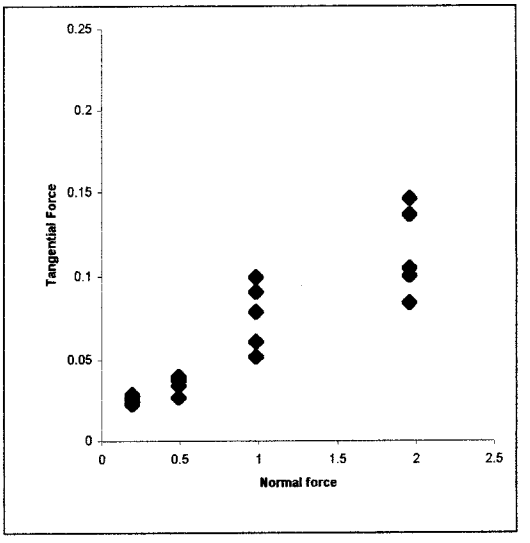

Figure 9: The friction force versus normal force data for heavy gold.

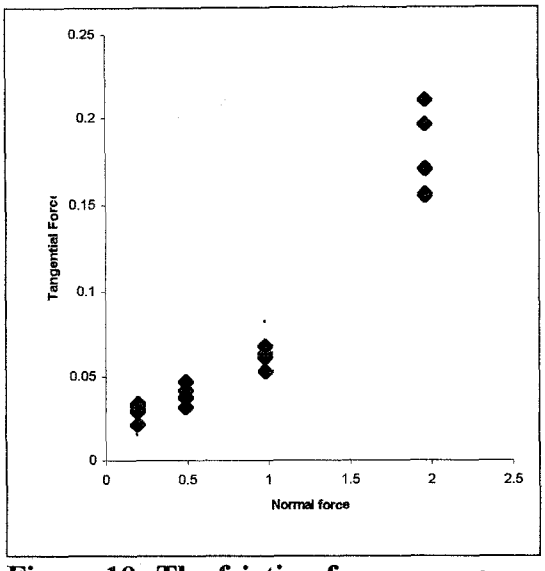

Figure 10: The friction force versus normal force data for flash gold.

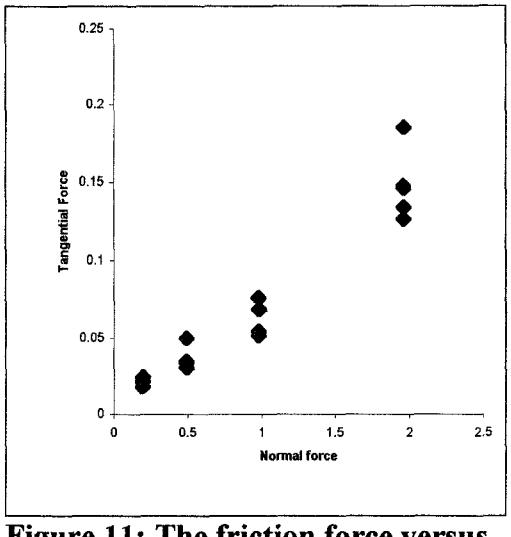

Figure 11: The friction force versus normal force data for WE#1 over R156.

upper and lower values for gold lie outside the intervals for the other two systems. Therefore, it is likely that the dynamic coefficient of friction for the heavy gold system is different from the other two systems. The upper and lower bounds for the flash gold and WE#1 over R156 coincide. Therefore, no statistical difference is detected.

The values presented in Table 4 are similar to previously published data [6]. During fretting debris is produced and causes some rolling to take place [6]. Waterhouse notes that rolling friction values are about 0.002 [6]. His values were about 0.05 [6]. So he theorized that some sliding was taking place [6].

5.0 Surface Examination and Discussion

The wear tracks were examined using a light metallograph. Since the same material was on each surface, material transfer was expected to occur from the flat to the rider. In all cases, material appeared to be transferred from the flat component to the rider.

No discernable wear was detected on the flash gold (GF PdNi) samples after fretting at 20 grams. The gold remained intact on both contact surfaces. After fretting at 50 and 100 gram loads, the flash was worn off the "flat" surface. Gold was worn off both surfaces at 200 grams.

For the clad WE#1 over R156 samples, the contact surface remained WE#1 to WE#1 at normal loads of 20, 50 and 100 grams. R156 was exposed after fretting at 200 grams.

Table 4: The dynamic coefficient of friction values and a 95% confidennce interval

Material System	$\mu_{dynamic}$	Confidence Interval	
		Lower	Upper
Heavy Gold	0.052	0.04	0.064
Flash Gold	0.086	0.072	0.099
WE#1 over R156	0.069	0.065	0.074

The metallographic observations were confirmed using nitric acid vapors. Nitric acid attacks both Pd-Ni and R156. The corrosion products have a distinct dark brown to black color.

The results for the clad WE#1 over R156 system and the gold flash (GF PdNi) system are consistent with previous findings [7,8]. At 20, 50 and 100 gram loads, the thin gold flash and WE#1 layers provided lubrication. This benefit is evident in both Fig. 10 and Fig. 11. The tangential forces for both systems were nearly identical in this load range. At 200 grams, the gold flash was rapidly worn away, typically within the first few hundred cycles whereas the WE#1 layer has proven to be more durable. Under identical load and motion conditions, the contact interface of a WE#1over R156 system remains WE#1-WE#1 long after the contact interface of a GF PdNi system has eroded from Au-Au to Au-Pd to PdNi-PdNi. The result was a lower average tangential load at 200 grams for the WE#1 over R156 system when compared to the gold flash system.

The contact interface on the heavy gold system remained gold-gold after fretting at all contact loads. The microstructure of cobalt hardened electroplated gold is not comparable to either PdNi or WE#1 over R156. Whereas the latter are true metals, electroplated hard gold is composite and can best be described as fine gold grains with a cobalt metal organic complex in the grain boundaries. The organic compound lowers the interfacial shear strength of the asperity junctions resulting in lower tangential forces.

No frictional polymers were detected during the material study. This is probably due to the fact that the experiments were conducted in a very dry environment, free of polmer forming contaminants.

6.0 Conclusions

The purpose of this research project was to explore the tendency for a material system to form a strong metallic bond (stick) during fretting conditions. The dynamic coefficient of friction was chosen as a figure of merit to differentiate between material systems. In addition, a mathematical model for the constant force-fretting machine was developed. This model was used to calculate the dynamic coefficient of friction for the material systems. Three different material systems were compared based on their tendency to form strong metallic bond (stick) and on their dynamic coefficient of friction.

Four different normal forces were used during this research project. The fret amplitude of the pseudo-crossed rod configuration was monitored and data were collected on fret amplitude using a laser displacement meter. The number of cycles required to cause fret amplitude to decrease to zero (stick) were recorded for all five of the replications at each normal force.

The heavy gold system endured more fretting cycles before the pseudo-crossed rods stopped moving and had the lowest calculated dynamic coefficient of friction. Under the fretting conditions presented in this paper the heavy gold system is preferred over the over two material systems. Although WE#1 over R156 endured more fretting cycles before sticking and had a lower dynamic coefficient of friction than the flash gold system, the differences were not statistically significant in this experiment.

7.0 References

[1] Holm, R., Electric Contacts Handbook, Springer-Verlag, Berlin, 1958.

[2] Seely, F., Smith, O., Resistance of Metals, John Wiley and Sons, New York, 1956.

[3] Hardee, H. and Aukland, N. "A New Constant Force/Displacement Fretting Test Machine," Proceedings of the 17th International Conference on Electrical Contacts, pp 17-24, 1994.

[4] Aukland, N., Leslie, I., Hardee, H., Lees, P. "A Statistical Comparison of a Clad Material and Gold Flashed Palladium Nickel Under Various Fretting Conditions", Proceedings of the Forty-First Holm Conference on Electrical Contacts, pp 52-63, 1995.

[5] Bryant, M. "Assessment of Fretting Failure Models of Electrical Connectors", Proceedings of the Fortieth Holm Conference on Electrical Contacts, 1994, pp 167-175.

[6] Waterhouse, R.B., Fretting Corrosion, Pergamon Press, 1972.

[7] Lees, P.W., "A Comparison of Electroplated Gold Flashed Palladium-Nickel and Wrought Clad Inlay WE#1 Capped Palladium-Silver", Proceedings of the 28th Annual Connector and Interconnection Symposium, pp 363-379 1995.

[8] Lees, P.W., "Fretting Behavior of Gold Flashed Palladium, Palladium Nickel and Palladium Silver Contact Materials", Proceedings of the Thirty Seventh Holm Conference on Electrical Contacts, pp 203-215, 1991.

[9] Martin, J.B., Thornton, S.T., Classical Dynamics of Particles and Systems, Harcourt Bruce College Publishers, 1995.

APPENDIX 1.

The system is driven sinusoidally at an angular frequency, w. We assumed that the system motion occurs at the angular frequency of the driving force and we ignored any phase shifting between the applied force and the position. Thus, the position, velocity, and acceleration are given by:

$$x = A \cdot \sin(w \cdot t) \quad (1)$$

$$v = A \cdot w \cdot \cos(w \cdot t) \quad (2)$$

$$a = -A \cdot w^2 \cdot \sin(w \cdot t) \quad (3)$$

The forces in the system can be separated into three components: the applied force from the electrodynamic driver, the resistive force due to the inherent friction in the dynamic system, and the friction force due to the fretting contact between the two pseudo-crossed rods. In addition to these forces, there is an additional inertial effect (mass times acceleration) because of non-zero accelerations given by Equation (3). Assuming that the friction force is a sinusoid (rather than constant), the sum of forces can be written as:

$$F_{applied} \cdot \sin(w \cdot t) - F_{damping} \cdot \sin(w \cdot t) - F_{friction} \cdot \sin(w \cdot t) = m \cdot a \quad (4)$$

or

$$F_{applied} \cdot \sin(w \cdot t) - F_{damping} \cdot \sin(w \cdot t) - F_{friction} \cdot \sin(w \cdot t) = m \cdot [-A \cdot w^2 \cdot \sin(w \cdot t)] \quad (5)$$

Note that all the sinusoids cancel, so only the amplitudes are left.

$$F_{applied} - F_{damping} - F_{friction} = m \cdot [-A \cdot w^2] \quad (6)$$

Solving for the friction due to fretting:

$$F_{friction} = m \cdot [-A \cdot w^2] + F_{applied} - F_{damping} \quad (7)$$

The mass, amplitude of motion, and frequency of vibration of the system are known, but the remaining terms: applied force and damping response are not.

Determining these last two terms requires additional information about the system that can only be found through additional measurements or modeling of the system.

To determine the force applied to the system based on our measured voltage values, we must know how fret amplitude is affected by changes in voltage applied to the electrodynamic drivers. We believed that this relationship was linear. Therefore, we examined the system without any friction load, such that there wasn't any contact with the fretting surface. At increasing voltages to the driver, we measured the resulting amplitude of the unloaded system. Figure A contains the resulting plot:

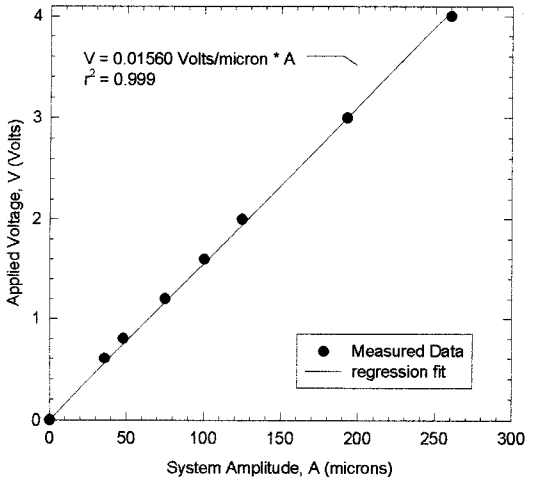

Figure A: The relationship between the voltage applied to the system and the fretting amplitude.

The relationship is of the form

$$V = c_{1free} \cdot A_{free} \qquad (8)$$

where the slope, $c_{1free} = 0.0156$ Volts /micron, A is the peak to peak amplitude of the sinusoidal motion, and V is the voltage applied to the system. The subscript "free" is to denote that the system does not have any load due to friction. We also note that the results were extremely linear, confirming our early expectations.

The amplitude of the motion during fretting will be less than the amplitude when there is no friction due to fretting. This decrease in amplitude will be due to the forces exerted by friction at the fretted surfaces. Based on Equation (8), we know that fret amplitude depends on the voltage sent to the driver. To determine the forces in the system, we must know how the applied force depends on the voltage presented to the electrodynamic drivers. We decided against taking the fretting system apart to measure these forces directly as the voltage is increased. Instead we chose to model the system. From this model, we expected to develop a relationship between driving force and fret amplitude. The equation for this relationship would then be substituted into Equation (8) to find the Voltage-Force equation.

To model this relationship, the mass of the rod and the spring constant of the system was needed. The mass of the rod was 0.125 kg. To find the spring constant of the system, a force was applied to the rod via a spring whose spring constant was already measured. Figure B contains the data collected to determine the displacement force relationship.

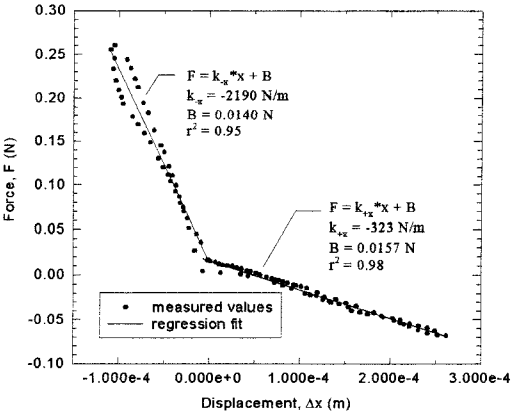

Figure B: The determination of the spring constant for the system.

The spring constant was found to have two values: -323 N/m for positive displacements, and -2190 N/m for negative

displacements. The system was tested for hysterysis effects, and only minor hysterysis was observed. An unexpected outcome of these measurements was that the spring constant depended on the direction the force was applied. Examining the system further, we found that each spring consisted of two membranes. One membrane acted on displacements away from the driver, while both membranes affected displacements into the driver. Thus, two separate spring constants were produced that were dependent on the direction of displacement.

Because the mechanical system under study quickly comes to rest after a displacement, the system must be loosing energy to internal friction, which is called damping. Finding the amount of this damping, denoted β, is important to simulate the system correctly. Further, the damping and the spring constants determine the resonance frequency of the system. A damped system with no external forces can be modeled as:

$$\ddot{x} + 2 \cdot \beta \cdot \dot{x} + \frac{k}{m} \cdot x = 0 \qquad (9)$$

[9].

Note that the damping term effectively provides a force proportional to velocity. If the damping constant is small, the system may be underdamped and tend to oscillate like a spring before coming to rest. If it is overdamped, it will stop without any oscillation. Examination of our system reaction after a displacement indicated that our system was overdamped. The solution to Equation (9) for overdamping and a constant k is well known:

$$x(t) = e^{-\beta t} \cdot \left[A_1 \cdot e^{w_2 t} + A_2 \cdot e^{-w_2 t} \right]$$
$$w_2 = \sqrt{\beta^2 - \frac{k}{m}} \qquad (10)$$

[9].

We approximated our system assuming a constant k value to use this solution. To determine this k value, the spring constant values in each direction were averaged, such that $k/m \sim 10000/sec^2$. Using experimental data collected from the system and then fitting the data to Equation 10, we obtained β values of 119.5, 117.4, and 121.9 sec^{-1}. The average, 119.9 sec^{-1}, was used as the damping factor for the system.

After the spring constant and damping factor are known, the system is ready to be modeled. With the sinusoidal driving force added, the system model becomes:

$$\ddot{x} + 2 \cdot \beta \cdot \dot{x} + \frac{k}{m} \cdot x = \frac{F_0}{m} \cdot \cos(w \cdot t) \qquad (11)$$

[9].

Euler integration techniques were used to model the system. A computer program was written to aid in the simulation of the system. The solution to the differential Equation (11) has two parts: the particular solution and general solution, which correspond to the initial behavior and steady state behavior of the system. The steady state solution of the system is at the frequency of the driving force. This supports our initial assumptions in Equations (1-3) that the displacement, velocity, and acceleration would all be at frequencies corresponding to only the driving frequencies.

The system was simulated at four Hz with 1,000 time steps per cycle. We confirmed convergence of solutions using 10,000 time steps per cycle, which produced the same results. As the resulting displacements versus time were graphed, we noted the number of cycles required to allow the steady state solution to became dominant. We called the magnitude of the motion after this time the steady-state amplitude of the system. This generally occurred in 2 to 3 cycles of motion. We then simulated the system with increasing driver force, and noted the resulting steady-state amplitude of the system. The results of this simulation give a relationship such that

$$A_{free} = c_{2\,free} \cdot F_{applied} \quad (12)$$

Data fitting Equation (12) was plotted in Figure C in order to measure c_{2free}.

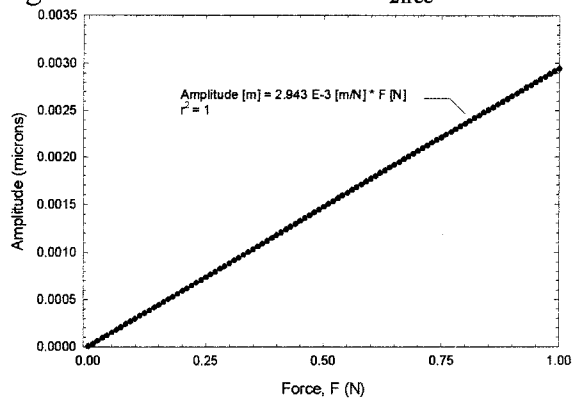

Figure C: The graph of system amplitude versus applied force for the free-motion system.

C_{2free} was determined to be 2.943 x 10^{-3} m / N. We now have a relationship between the applied voltage to the driver and the force exerted by the driver,

$$F_{applied} = F_0 = \frac{V}{c_{1\,free} \cdot c_{2\,free}} \quad (13)$$

At this point, the friction force as shown in Equation (7) is almost known. However, the system response, $F_{damping}$ is unknown. Again, we can use the simulation to obtain a relationship between system response and the fretting amplitude. The relationship between Amplitude, A, and system force, $F_{damping}$, was found to be:

$$F_{damping} = c_{3free} \cdot A \quad (14)$$

Where c_{3free} = -2.596 x 10^{-4} N/micron. We can now determine the friction force from Equation (7),

$$F_{friction} = M \cdot A \cdot w^2 + \frac{V}{c_{1\,free} \cdot c_{2\,free}} - \frac{A}{c_{3\,free}} \quad (15)$$

where M is the mass of the moving system, A is the amplitude, V is the voltage applied to the system, and c_{1free}, c_{2free}, and c_{3free} are the constants previously discussed.

Using this equation for the friction force, we can determine the coefficient of friction for each material system.

$$\mu_{dynamic} = \frac{F_{friction}}{N} \quad (16)$$

where $\mu_{dynamic}$ is the dynamic coefficient of friction, $F_{friction}$ is the friction force, and N is the normal force on the plate.